Available online at www.sciencedirect.com

ScienceDirect

Proceedings of the Combustion Institute 35 (2015) 3497–3504

Proceedings of the Combustion Institute

www.elsevier.com/locate/proci

Effect of non-equilibrium plasma on two-stage ignition of *n*-heptane

Sharath Nagaraja *, Wenting Sun, Vigor Yang

School of Aerospace Engineering, Georgia Institute of Technology, Atlanta, GA 30332, USA

Available online 26 June 2014

Abstract

The effect of pulsed nanosecond dielectric barrier plasma discharges on the ignition characteristics of n-heptane and air mixtures is investigated through self-consistent simulations in a plane-to-plane geometry at reduced pressures (20.3 kPa). The present work represents one of the first attempts in understanding the kinetic and thermal effects of nanosecond pulsed discharges on the two-stage ignition process of n-heptane. A plasma-fluid formulation is developed with ions and neutral species at gas temperature, and electrons in non-equilibrium. The work makes use of an optimized chemical kinetics mechanism consisting of 166 species and 611 reactions, obtained by combining a reduced n-heptane kinetic model, a non-equilibrium plasma chemistry scheme, and a NO_x kinetic model. The catalytic effect from plasma-generated radicals on the first stage of the n-heptane ignition process has been identified. Production of radicals such as O, H and OH from the plasma initiates and accelerates the H abstraction of fuel molecules, and dramatically reduces the induction time of the exothermic cycle ($RH \rightarrow R \rightarrow RO_2 \rightarrow OROOH$) by a factor of 10. Furthermore, the plasma action on low temperature chemistry is found to be nearly independent of the equivalence ratio and more pronounced at lower temperatures (550–650 K). A staggered application of nanosecond voltage pulses (2–4 pulses at the beginning and 20–30 pulses after the first stage heat release) is shown to be optimal, resulting in a reduction of the ignition delay by approximately a factor of 2. NO production from the plasma via electron impact and quenching processes at low temperatures plays an important role in promoting chain-branching reactions and contributes to shortening the ignition delay by approximately 10%.

Keywords: Plasma assisted combustion; Low temperature chemistry; Ignition; N-heptane

1. Introduction

Non-equilibrium plasma discharges have recently drawn considerable attention as a promising technology for combustion enhancement in air-breathing engines [1–3]. A variety of experimental platforms and measurement techniques have been developed to understand the complex mechanisms involved in the interactions between plasma and combustion [1–10]. Both experimental and numerical studies have been conducted to explore the effects of plasma-generated species on ignition [2,5,10,11], flame stabilization [7,8], flame speed enhancement [12,13], and extinction [14,15].

* Corresponding author.
E-mail address: sharath@gatech.edu (S. Nagaraja).

http://dx.doi.org/10.1016/j.proci.2014.05.123
1540-7489/

Yu Starikovskii and co-workers [5,16] reported that application of a nanosecond pulsed discharge in a fuel–air mixture in a shock tube could reduce ignition delay times of C_1–C_5 saturated hydrocarbons by approximately one order of magnitude. This phenomenon was attributed to the breaking of C–C bonds in fuel molecules by the plasma-generated radicals such as atomic oxygen (O) [16]. Recent studies on the ignition of H_2–air mixtures subjected to nanosecond pulsed plasma [10,11] demonstrated that the local plasma chemistry expedites the transition of the mixture to the ignition threshold, with heat transport playing a minor role. Ombrello et al. experimentally explored the enhancement of C_2H_4 and C_3H_8 flame propagation by singlet oxygen ($O_2(^1\Delta_g)$) and ozone (O_3) [12,13]. Sun et al. [15] integrated an *in situ* nanosecond pulsed discharge system with a counterflow burner. It was found that the production of radicals, especially atomic oxygen, from the plasma can dramatically change the reaction pathways of CH_4, thereby modifying both ignition and extinction characteristics. Nanosecond discharges have also been employed to improve the stability of bluff-body anchored lean premixed flames for CH_4 and C_3H_8, mainly due to radical production [7] and local fuel reforming [8].

Owing to the complexity of plasma/chemistry interactions and lack of a reliable kinetic database, most of the previous work in this area has focused on hydrogen or small hydrocarbon fuels (C_1–C_5). There is a lack of comparison between plasma assisted ignition of C_1–C_5 and larger hydrocarbon (C_6 and above) fuels. The latter feature rich low-temperature chemistry which is weak or completely absent in small hydrocarbon fuels [17]. Motivated by this observation, the objective of this study is to numerically investigate the effect of non-equilibrium plasma on ignition properties of n-heptane (nC_7H_{16}), for which low-temperature chemistry plays a critical role. No experimental data is currently available in the literature on non-equilibrium plasma-assisted ignition of large hydrocarbons, such as nC_7H_{16}. The present numerical study represents one of the first attempts in understanding the kinetic and thermal effects of nanosecond pulsed discharges on the two-stage ignition process of nC_7H_{16}. The kinetic and thermal effects of nanosecond pulsed discharges on the two-stage ignition process of nC_7H_{16} will be studied in detail. In addition, the catalytic effects of plasma-generated NO_x on the ignition process will be examined.

2. Model framework

2.1. Physical configuration

Figure 1 shows schematically the physical configuration considered herein. Two copper electrodes are placed in a parallel plate configuration, each covered with a 1.75 mm quartz layer (dielectric constant, $\varepsilon_g = 3.8$). The gap between the dielectric boundaries (0.25 cm) is filled with a mixture of pre-vaporized nC_7H_{16} and dry air (79% N_2 and 21% O_2) at 20.3 kPa with the equivalence ratio and initial temperature in the range of 0.5–1.5 and 550–650 K, respectively. Gaussian voltage pulses (peak voltage of 20 kV and pulse duration of 40 ns) are applied at the right electrode, whereas the left electrode is grounded. The pulse repetition frequency is fixed at 60 kHz. We have shown in our previous work [11] that under this condition, one-dimensional approximation is sufficient to self-consistently simulate the nanosecond plasma dynamics and the development of the ignition kernel.

2.2. Governing equations

The details of the theoretical formulation and numerical model used in the present work are described in [18]. Only a brief summary is given here. Governing equations for electric potential, electron energy, and charged and neutral species continuity are considered. In addition, the conservation equations of mass, momentum and energy for the gas mixture are solved simultaneously to treat flow motion. The electron transport and reaction coefficients are expressed as functions of electron energy using BOLSIG [19] and updated at every time step through interpolation. An adaptive time-step approach is utilized to tackle the large disparity in the timescales of the various physical phenomena of interest. Implicit time integration is performed for stiff chemical source terms, whereas species and flow transport are treated explicitly for computational efficiency. A non-uniform mesh consisting of 300 grid points, with highest resolution near the two dielectric boundaries, is used to obtain grid convergent solutions. A domain decomposition approach with MPI (message passing interface) is implemented to compute the solution in parallel over multiple processors.

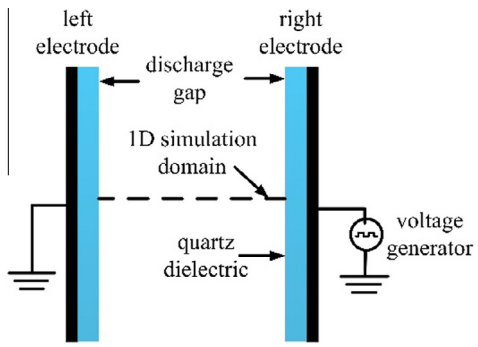

Fig. 1. Schematic of the dielectric barrier discharge cell.

The predictive capability of the numerical code has been well validated with measurements of the input electrical energy, atomic oxygen and temperature in nanosecond pulsed plasma in air [11]. In addition, the model was benchmarked against experimental data on temperature, OH and ignition delay in H_2–air mixtures subjected to pulsed nanosecond discharges [18].

2.3. Kinetic models of nC_7H_{16} and air plasma

In order to understand the effect of radicals generated by pulsed discharges on the low- and high-temperature chemical pathways in the ignition of nC_7H_{16}, an optimized kinetic model is developed. The scheme combines a reduced nC_7H_{16} chemical kinetic model [17,20] fuel and air plasma reactions [21,22] and NO_x reactions [23,24]. The entire scheme consists of 166 species and 611 reactions, incorporating charged species N_2^+, O_2^+, HN_2^+, H_3O^+, $C_7H_{15}^+$, $C_6H_{13}^+$, $C_5H_{11}^+$, O_2^-, and e^-; excited species $N_2(A^3)$, $N_2(B^3)$, $N_2(C^3)$, $N_2(a^1)$, and $O(^1D)$; and neutral species. Electron impact processes (ionization, dissociation, excitation and attachment) along with quenching, detachment and recombination reactions are considered. The rate coefficients of electron-based reactions are calculated at each instant (at every spatial node) by solving the electron Boltzmann equation with two-term expansion using the BOLSIG software [19]. For this purpose, self-consistent sets of electron impact cross-sections are used for O_2 [25] and N_2 [26]. There are, however, no cross-section data available for nC_7H_{16}. It is therefore assumed that the cross-section for nC_7H_{16} is similar to that of C_2H_6 taken from [27]. A sensitivity analysis was conducted by varying (up to 5 times) the rate constants of electron impact and quenching reactions of nC_7H_{16}. Negligible impact on ignition delay predictions was found.

NO_x kinetics (from GRI Mech 3.0 [23]) is included in the kinetic model to study the catalytic effect of NO on ignition [4]. Plasma can efficiently generate *NO* through the following pathways [24],

$$N_2 + e \rightarrow N(^2D) + N + e \quad (1)$$

$$N(^2D) + O_2 \rightarrow NO + O \quad (2)$$

$$N_2(A^3) + O \rightarrow NO + N(^2D) \quad (3)$$

Takita et al. [24] and Ombrello and Ju [4] demonstrated that NO can have a catalytic effect on hydrocarbon fuel ignition via reactions 4–7, which have also been included in the present kinetics mechanism,

$$NO + HO_2 \leftrightarrow NO_2 + OH \quad (4)$$

$$CH_3 + O_2 + M \leftrightarrow CH_3O_2 + M \quad (5)$$

$$CH_3O_2 + NO \leftrightarrow CH_3O + NO_2 \quad (6)$$

$$CH_3 + NO_2 \leftrightarrow CH_3O + NO \quad (7)$$

3. Results and discussion

Application of a nanosecond voltage pulse in a mixture of nC_7H_{16} and air (equivalence ratio, $\phi = 1.0$, $p = 20.3$ kPa, $T = 600$ K) causes electrical breakdown at ~5.5 kV, resulting in a surge in the conduction current as shown in Fig. 2. Charge accumulation on the dielectric layers shields the plasma from further increase in applied voltage, and a rapid fall in current is observed. The E/N ratio in the entire discharge gap is calculated self-consistently for each voltage pulse from the electric field obtained by solving the Poisson equation. The E/N ratio at the center of the discharge volume is also shown as a function of time in Fig. 2. The total input energy is found to be ~0.6 mJ per pulse. It is evident that a significant portion of the input pulse energy is coupled at E/N values greater than 100 Td, resulting in rapid electron impact dissociation, excitation and ionization of neutral species.

3.1. Plasma species production

The reactive species generated by the plasma have a critical effect on the nC_7H_{16} ignition properties. Figure 3 shows the mole-fractions of O, H, OH and NO and temperature profiles after a burst of 5 voltage pulses (at 0.1 ms) at 60 kHz pulsing frequency as a function of distance from the left electrode. The E/N ratio after 5 ns from the beginning of the 5th pulse is also shown to facilitate discussions. Atomic oxygen is predominantly produced via electron impact dissociation of O_2, and quenching of excited N_2 by O_2. Two small peaks are noticed in the spatial profile of the O

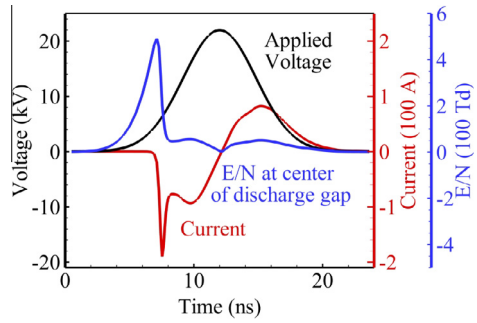

Fig. 2. Applied voltage, current and E/N at the center of the domain as a function of time during a discharge pulse in a n-C_7H_{16} and air mixture ($\phi = 1.0$, $P = 20.3$ kPa, $T = 600$ K).

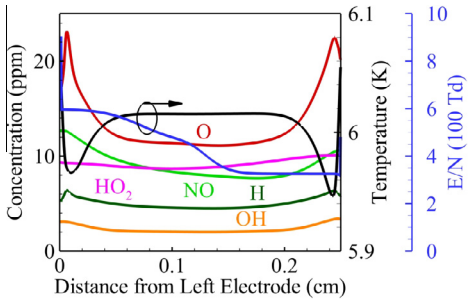

Fig. 3. Spatial distribution of O, H, OH, NO and HO_2 concentrations and temperature after 5 discharge pulses in a nC_7H_{16} and air mixture ($\phi = 1.0$, $P = 20.3$ kPa, $T = 600$ K). E/N profile after 5 ns from the beginning of the 5th discharge pulse is also shown.

atom near the boundaries, where the mole-fraction is ~2 times the value at the center. This behavior can be attributed to higher E/N and electron densities during breakdown, near the boundary sheath edges, as compared to corresponding values in the bulk plasma region. As a result, the electron impact dissociation and excitation rates are higher near the boundaries than at the center of the discharge gap. The H atom exhibits trend similar to that of O, and is produced via electron impact dissociation and quenching reactions of nC_7H_{16}. The H mole-fraction, however, is ~5 times lower than that of O because the concentration of nC_7H_{16} (0.019 mol-fraction) is much smaller than the concentration of O_2 (0.2 mol fraction) under the present operating conditions. The relatively low average temperature of 600 K favors generation of HO_2 via three-body reactions between H and O_2 in the discharge volume. The concentration of NO in the discharge volume is ~10 ppm after 6 pulses, and is produced by the plasma via reactions 1–3. The effect of NO on the ignition kinetics will be discussed later in more detail. OH radicals can be produced by the reaction between HO_2 and NO (Eq. (4)), but results predominantly from the following reactions,

$$O + HO_2 \leftrightarrow OH + O_2 \quad (8)$$

$$H + HO_2 \leftrightarrow OH + OH \quad (9)$$

3.2. Effect of plasma on low temperature nC_7H_{16} chemistry

Figure 4 shows the temporal evolution of temperature at the center of the computational domain with and without the application of nanosecond discharge pulses. The operating conditions are the same as in Fig. 2. It is evident that pulsed nanosecond plasma accelerates the onset of the first-stage temperature rise (from 600 K to 800 K) nearly 10 times, from ~0.3 s (in the case of auto ignition) to ~35 ms (for 5 discharge pulses). The radicals generated by the plasma initiate the H abstraction from fuel molecules through the following and similar reactions,

$$nC_7H_{16} + OH/O/H \rightarrow n - C_7H_{15} + H_2O/OH/H_2 \quad (10)$$

For comparison, 2 and 8 pulses are applied to initiate the first stage of the nC_7H_{16} ignition process. It is observed that the plasma enhancement is a weak function of the number of pulses, and the difference is ~5%. This behavior can be attributed to the "self-acceleration" of the low temperature chain branching after some alkyl radicals, R, have been generated. As shown in Fig. 5, the alkyl radical triggers an exothermic cycle through the formation of RO_2, which isomerizes and adds another O_2 to form alkylperoxide O_2ROOH, followed by partial decomposition to smaller hydrocarbons, aldehydes and radical species such as OH and HO_2 [28,29]. These radicals further accelerate the initial H abstraction step, thereby creating a positive feedback loop. The nanosecond plasma acts as a catalyst by providing a small amount of seed radicals to initiate this "self-accelerating" process, and the quantity of radicals introduced initially is not of critical importance. A small amount of radical addition at low temperature conditions can dramatically change the time scales of low temperature kinetics.

The ignition delay time for nC_7H_{16} comprises the initiation time for the first-stage temperature rise and the intermediate induction period prior to the thermal explosion. The effect of the equivalence ratio on the plasma enhancement is shown in Fig. 6(a), which depicts the temperature rise at the center of the discharge gap as a function of time. The simulations were conducted at 600 K and 20.3 kPa with $\phi = 0.5$, 0.75, 1.0, 1.25 and 1.5, respectively. In each case, 5 discharge

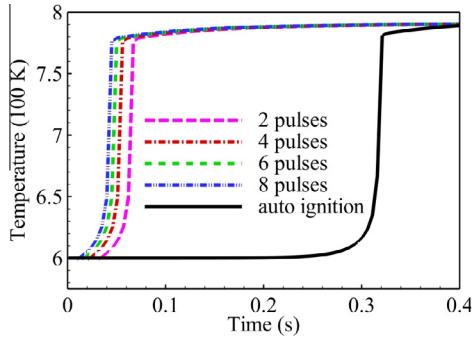

Fig. 4. Temporal evolution of temperature at the center of the discharge gap for cases with no plasma (auto-ignition), and for 2, 4, 6 and 8 discharge pulses applied at the beginning of the corresponding simulations ($\phi = 1.0$, $P = 20.3$ kPa, and $T = 600$ K).

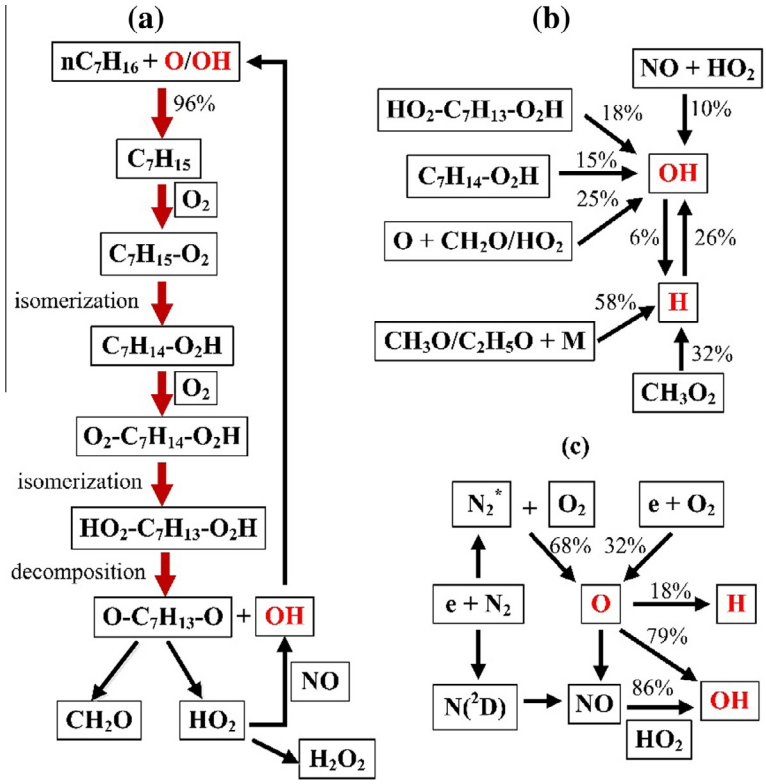

Fig. 5. Path flux analysis describing the first stage heat release. (a) nC_7H_{16} consumption, (b) OH and H formation, and (c) O production and consumption pathways ($\phi = 1.0$, $P = 20.3$ kPa, and $T = 600$ K).

pulses were applied at the beginning of the simulation. The corresponding auto-ignition curves are also shown for comparison. The plasma enhancement of the 1st stage is identical in each case, suggesting that the addition of radicals has a strong impact on the initiation time, irrespective of the equivalence ratio. It is worth noting that the temperature rise at the first ignition stage is higher in the case of rich mixtures. This behavior can be attributed to the large number of fuel molecules undergoing exothermic isomerization and decomposition reactions at higher equivalence ratios. The overall ignition delay is shorter for rich mixtures, regardless of plasma, because of the smaller induction period after the first-stage temperature rise. To further clarify the discussion, Fig. 6(b) shows the first- and second-stage ignition delay times as a function of equivalence ratio, for identical operating conditions as in Fig. 6(a). It is evident that application of 5 ns voltage pulses at the beginning of the simulation significantly reduces the first-stage ignition delay, and the magnitude is independent of the equivalence ratio. On the other hand, the discharge pulses applied at the beginning have negligible impact on the second-stage ignition delay.

Since the kinetic reaction pathways of nC_7H_{16} are highly temperature sensitive, the plasma enhancement is also studied at different initial temperature conditions. Figure. 7 shows the temperature evolution at the center of the discharge gap with initial temperatures of 550, 575, 600 and 650 K, respectively. The simulations were conducted for stoichiometric nC_7H_{16}–air mixtures at 20.3 kPa. The corresponding auto-ignition curves are also shown for comparison. At 550 K, the initiation time for the first-stage temperature rise constitutes a major portion of the overall ignition delay. In this case, application of only 5 discharge pulses at the beginning reduces the ignition delay by 70%, from 4.5 to 1.5 s. With increase in initial temperature, the initiation time decreases but the induction period increases. Hence, the impact of plasma in terms of percentage reduction in the ignition delay decreases. At a higher initial temperature (above 650 K), the initiation time is negligible compared to the ignition delay. Application of nanosecond discharge pulses at the beginning has negligible impact under this condition. It is of interest to understand the effect of discharge pulses after the first-stage heat release on the overall ignition delay times.

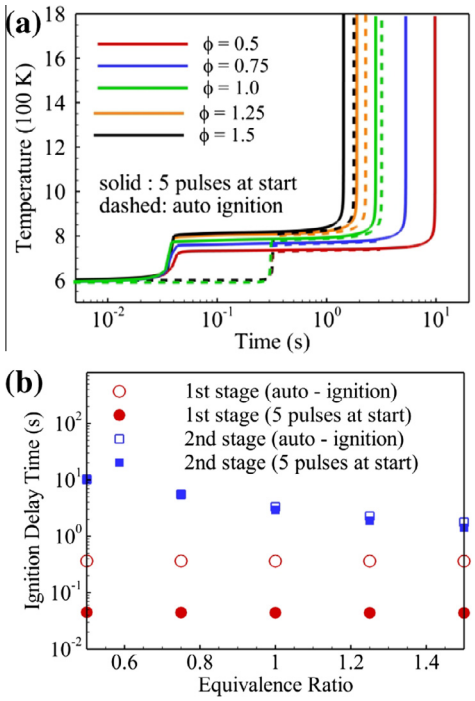

Fig. 6. (a) Temporal evolution of temperature, and (b) ignition delay times at the center of the discharge gap with and without 5 discharge pulses applied at the beginning of the corresponding simulations at 20.3 kPa and 600 K for $\phi = 0.5$, 0.75, 1.0, 1.25 and 1.5.

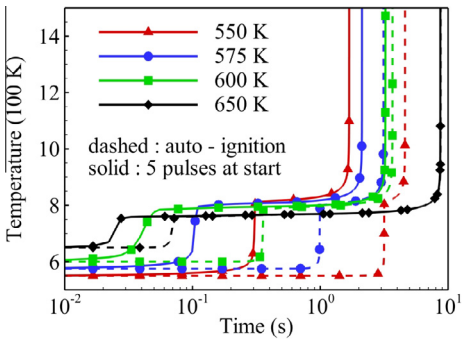

Fig. 7. Temporal evolution of temperature at the center of the discharge gap with and without 5 discharge pulses applied at the beginning of the corresponding simulations at 20.3 kPa and $\phi = 1.0$ for initial $T = 550$ K, 575 K, 600 K and 650 K.

3.3. Effect of staggered application of nanosecond pulses on Ignition of nC_7H_{16}

A staggered application of discharge pulses is found to have the greatest effect on the ignition delay time at low initial temperatures (below 800 K). A few pulses (2–6) are first applied at the beginning of the event, and the high voltage pulser is then switched off. The seed radicals generated by the plasma greatly accelerate the first-stage temperature rise. At this juncture, the pulser is switched on and a larger number of discharge pulses (5–20) are applied to further reduce the induction time of nC_7H_{16} ignition.

Figure 8 shows the temperature evolution at the center of the discharge gap, demonstrating the effect of staggered application of discharge pulses on the ignition delay. All the simulations were conducted for a stoichiometric nC_7H_{16}–air mixture at an initial pressure and temperature of 20.3 kPa and 600 K, respectively. For comparison, the temperature evolution without plasma (auto ignition) and with 5 discharge pulses applied at the beginning are included. The staggered pulsing consists of 5 pulses applied at the beginning, with the remaining pulses applied at 0.2 s after the first-stage temperature rise. Application of 6, 8 and 10 pulses in a staggered mode reduces the ignition delay by approximately 3%, 5% and 10%, respectively. This behavior suggests that the second- stage of the nC_7H_{16} ignition process is sensitive to the number of pulses in the burst (applied after the first stage).

Figure 9 shows the temperature evolution at the center of the discharge domain with 15 voltage pulses applied at the beginning, after the first ignition stage, and in a staggered mode, respectively. The auto-ignition curve is also included for comparison. All the simulations were conducted for a stoichiometric nC_7H_{16}–air mixture at an initial pressure and temperature of 20.3 kPa and 600 K, respectively. The effect of nanosecond discharges on the two-stage ignition process is highly dependent on how the voltage pulses are distributed in time. Application of 15 pulses at the beginning reduces the first-stage ignition delay by a factor of 10, but the overall ignition delay time drops only by 10% as compared to the auto-ignition

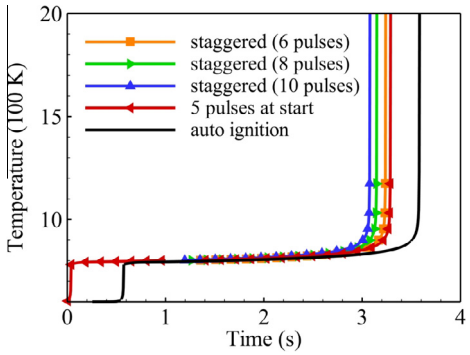

Fig. 8. Temporal evolution of temperature at the center of the discharge gap for case with no plasma (auto – ignition), 5 pulses applied at beginning, and staggered application of 6, 8 and 10 pulses, respectively ($\phi = 1.0$, P = 20.3 kPa, and $T = 600$ K).

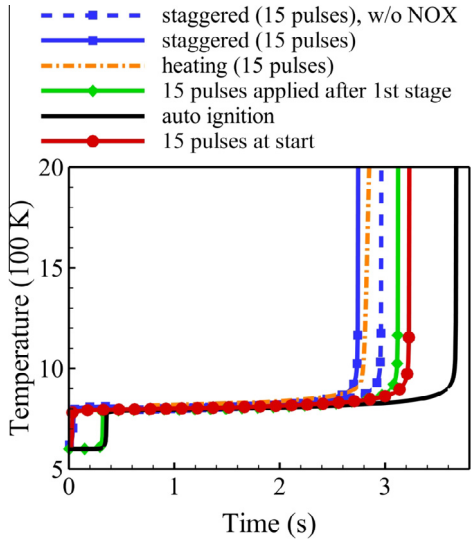

Fig. 9. Temporal evolution of temperature at the center of the discharge gap for cases with no plasma (auto – ignition), 15 pulses applied at the start, after 1st stage, and in a staggered mode. An additional case without NO_X kinetics is shown for staggered application of 15 pulses ($\phi = 1.0$, $P = 20.3$ kPa, and $T = 600$ K).

case. This can be attributed to the fact that the plasma has no impact on the long induction period after the first stage. On the other hand, application of the 15 discharge pulses after the first-stage temperature rise has an immediate impact on the induction period, and decreases the second-stage ignition delay by about 20%. The staggered application of 15 discharge pulses is most optimal and results in 30% reduction in the ignition delay as compared to the auto-ignition case.

Further analysis suggests that the plasma effect after the first-stage ignition is primarily thermal. For comparison, the result for 15 pulse thermal heating is included in Fig. 9. Five nonequilibrium discharge pulses are applied at $t = 0$, and thermal energy equivalent to the remaining 10 pulses is added after the first-stage ignition within the same time span. An additional source term is introduced in the energy equation whose magnitude is equal to the rate of energy addition in the case of a nonequilibrium discharge pulse. It is evident that thermal heating produces ignition delay similar to that with staggered application of 15 discharge pulses. Quenching of excited species and recombination of radicals generated by the plasma leads to a temperature rise of ~0.8 K/pulse. Application of 10 ns pulses during the induction period gives rise to a temperature rise of ~8 K within 0.5 ms. Higher temperatures promote faster decomposition of H_2O_2 to OH radicals. It is for this reason that increasing the number of pulses (increasing the heating rate) has a direct impact on reducing the induction time.

The energy added during each pulse is nearly the same (0.4–0.6 mJ). In the staggered mode, the time interval between two pulse bursts is 0.2 s. Ions generated in the first burst completely recombine before the beginning of the second burst. The plasma thermal effect can be attributed to the fast heat release from quenching of excited species generated during each pulse. Application of the same amount of thermal energy as that coupled during the discharge pulses before the first stage has negligible impact on the ignition delay. For example, the total energy of 15 pulse discharge is equivalent to that of a temperature rise of ~12 K. The initial temperature was raised artificially by 12 K, thereby resulting in a negligible reduction in the ignition delay.

The importance of including low temperature NO_x kinetics like reactions 4–7 is also shown in Fig. 9 for staggered application of 15 discharge pulses. Removing NO and NO_2 based reactions from the chemistry mechanism results in ~10% increase in the ignition delay. As mentioned in Section 2.4, nanosecond discharge pulses generate NO through reactions 1–3, whose rates are independent of the gas temperature. An analysis of reaction pathways (see Fig. 6) suggests that under low temperature conditions, nearly 86% of NO is consumed in reaction 4 with the remaining via reaction 5, to produce OH, which significantly accelerates H abstraction reactions of fuel molecules at low temperatures. The quantity of NO generated is proportional to the number of discharge pulses (approximately 1 ppm/pulse). Application of a larger number of pulses (50–100) may increase the NO concentration and the associated low-temperature catalytic effect will be more pronounced.

4. Conclusion

The effect of non-equilibrium, nanosecond pulsed plasma discharges on the ignition characteristics of nC_7H_{16} in air was studied by means of a self-consistent numerical analysis at a reduced pressure of 20.3 kPa. The plasma generated radicals initiated and significantly accelerated the H abstraction reaction from fuel molecules and triggered a "self-accelerating" feedback loop via low-temperature kinetic pathways. This behavior is in contrast to the reduction of the ignition delay of C_1–C_5 hydrocarbons by nonequilibrium discharges, which has been attributed to the breaking of C–C bonds by the plasma generated radicals [16]. Application of only a few discharge pulses at the beginning was sufficient to reduce the initiation time of the first-stage temperature rise by a factor of 10. The plasma effect on the low

temperature chemistry was independent of the equivalence ratio, but was more pronounced at lower initial temperatures (550–650 K). A staggered application of discharge pulses (a few pulses at the beginning and a larger number of pulses immediately after the first-stage temperature rise) was found to be optimal, reducing the ignition delay by nearly 40%. The plasma effect after the first stage was shown to be predominantly thermal. Temperature rise, introduced by quenching of excited species, radical induced fuel oxidation and radical/ion–electron recombination, accelerated the decomposition of H_2O_2 and reduced the induction period before ignition. NO produced by plasma pulses reacted with HO_2 to generate OH, which accelerated the low temperature nC_7H_{16} ignition.

This work also demonstrated that non-equilibrium plasma can dramatically modify the time scales of fuel kinetics, and therefore can be used to control the ignition timing for advanced engine technologies.

Acknowledgments

This work was supported by MURI research Grant FA9550-07-1-0136 from the Air Force Office of Scientific Research, with Dr. Chiping Li as the technical monitor. Wenting Sun is grateful for faculty startup support from the Georgia Institute of Technology.

References

[1] S.M. Starikovskaia, *J. Phys. D: Appl. Phys.* 39 (16) (2006) R265–R299.
[2] F. Wang, J.B. Liu, J. Sinibaldi, C. Brophy, A. Kuthi, C. Jiang, P. Ronney, M.A. Gundersen, *IEEE Trans. Plasma Sci.* 33 (2) (2005) 844–849.
[3] S.B. Leonov, D.A. Yarantsev, A.P. Napartovich, I.V. Kochetov, *IEEE Trans. Plasma Sci.* 34 (6) (2006) 2514–2525.
[4] T. Ombrello, Y. Ju, *IEEE Trans. Plasma Sci.* 36 (2008) 2924–2932.
[5] S.A. Bozhenkov, S.M. Starikovskaia, A.Y. Starikovskii, *Combust. Flame* 133 (2003) 133–146.
[6] M. Uddi, N. Jiang, E. Mintusov, I.V. Adamovich, W.R. Lempert, *Proc. Combust. Inst.* 32 (2009) 929–936.
[7] G. Pilla, D. Galley, D.A. Lacoste, F. Lacas, D. Veynante, C.O. Laux, *IEEE Trans. Plasma Sci.* 34 (6) (2006) 2471–2477.
[8] W. Kim, M.G. Mungal, M.A. Cappelli, *Combust. Flame* 157 (2) (2010) 374–383.
[9] W. Sun, M. Uddi, T. Ombrello, S.H. Won, C. Carter, Y. Ju, *Proc. Combust. Inst.* 33 (2011) 3211–3218.
[10] Z. Yin, I.V. Adamovich, W.R. Lempert, *Proc. Combust. Inst.* 34 (2013) 3249–3258.
[11] S. Nagaraja, V. Yang, Z. Yin, I.V. Adamovich, *Combust. Flame* (2013).
[12] T. Ombrello, S.H. Won, Y. Ju, S. Williams, *Combust. Flame* 157 (2010) 1906–1915.
[13] T. Ombrello, S.H. Won, Y. Ju, S. Williams, *Combust. Flame* 157 (2010) 1916–1928.
[14] W. Sun, M. Uddi, S.H. Won, T. Ombrello, C. Carter, Y. Ju, *Combust. Flame* 159 (2012) 221–229.
[15] W. Sun, S.H. Won, T. Ombrello, C. Carter, Y.Ju. Proc, *Combust. Inst.* 34 (1) (2013) 847–855.
[16] A. Yu Starikovskii, N.B. Anikin, I.N. Kosarev, E.I. Mintoussov, M.M. Nudnova, A.E. Rakitin, D.V. Roupassov, M.P. Burke, S.M. Starikovskaia, V.P. Zhukov, *J. Prop. Power* 24 (6) (2008) 1182–1197.
[17] Y. Ju, W. Sun, M.P. Burke, X. Gou, Z. Chen, *Proc. Combust. Inst.* 33 (2011) 1245–1251.
[18] S. Nagaraja, V. Yang, I.V. Adamovich, *J. Phys. D: Appl. Phys.* 46 (15) (2013) 155205.
[19] G.J.M. Hagelaar, L.C. Pitchford, *Plasma Sour. Sci. Tech.* 14 (4) (2005) 722.
[20] H. Seiser, H. Pitsch, K. Seshadri, W.J. Pitz, H.J. Curran, *Proc. Combust. Inst.* 28 (2000) 2029–2037.
[21] M. Uddi, N. Jiang, I.V. Adamovich, W.R. Lempert, *J. Phys. D: Appl. Phys.* 42 (7) (2009) 075205.
[22] N.A. Popov, *Plasma Phys. Rep.* 34 (5) (2008) 376–391.
[23] G.P. Smith, D.M. Golden, M. Franklach, et al., GRI-Mech 3.0, 1999, <http://www.me.berkeley.edu/gri_mech/>.
[24] K. Takita, N. Abe, G. Masuya, Y. Ju, *Proc. Combust. Inst.* 31 (2) (2007) 2489–2496.
[25] A.A. Ionin, I.V. Kochetov, A.P. Napartovich, N.N. Yuryshev, *J. Phys. D Appl. Phys.* 40 (2007) R25–R61.
[26] A.V. Phelps, L.C. Pitchford, *Phys. Rev. A* 31 (1985) 2932.
[27] M. Hayashi, in: L.C. Pitchford, B.V. McCoy, A. Chutjian, S. Trajmar (Eds.), *Swarm Studies and Inelastic Electron–Molecule Collisions*, Springer Verlag, New York, 1987, pp. 167–187.
[28] C.K. Westbrook, *Proc. Combust. Inst.* 28 (2) (2000) 1563–1577.
[29] S. Tanaka, F. Ayala, J.C. Keck, J.B. Heywood, *Combust. Flame* 132 (2003) 219–239.